



Microwave-assisted low temperature synthesis of wurtzite ZnS quantum dots

Robina Shahid*, Muhammet S. Toprak*, Mamoun Muhammed

Division of Functional Materials, Royal Institute of Technology (KTH), 16440, Kista, Stockholm, Sweden

ARTICLE INFO

Article history:

Received 26 November 2011

Received in revised form

30 December 2011

Accepted 2 January 2012

Available online 11 January 2012

Keywords:

Nanostructure

Semiconductors

Quantum dots

Microwave

Chemical synthesis

Optical properties

ABSTRACT

In this work we report, for the first time, on microwave assisted synthesis of wurtzite ZnS quantum dots (QDs) in controlled reaction at temperature as low as 150 °C. The synthesis can be done in different microwave absorbing solvents with multisource or single source precursors. The QDs are less than 3 nm in size as characterized by transmission electron microscopy (TEM) using selected area electron diffraction (SAED) patterns to confirm the wurtzite phase of ZnS QDs. The optical properties were investigated by UV–Vis absorption which shows blue shift in absorption compared to bulk wurtzite ZnS due to quantum confinement effects. The photoluminescence (PL) spectra of QDs reveal point defects related emission of ZnS QDs.

© 2012 Elsevier Inc. All rights reserved.

1. Introduction

Quantum dots (QDs) are nanocrystalline semiconductor materials that show quantum confinement effect when the nanoparticle radius is below the exciton Bohr radius and have typical diameters of 2–20 nm [1]. According to the wide variation of the dielectric constant and of the effective mass of the electron and the hole, the exciton Bohr radius in real semiconductors covers a fairly wide range; from 7 Å of CuCl to 100 Å of GaAs [2].

Since the basic experimental relationship between size and optical spectra was first established and confirmed for ZnS and CdS colloidal semiconductor nanocrystals (NCs) [3–5], numerous research has been carried out to synthesize colloidal semiconductor (NCs) and study their optical properties [6–10]. Due to size-dependent absorption and emission properties, narrow size distribution and high luminescent efficiency QDs are of great interest for their applications in biomedical labeling, light emitting diodes (LEDs), solar cells, lasers, and sensors [11].

Research in this field is quite wide and successful, but recent environmental regulations restrict the use of toxic metals [12]. New alternatives to Cd and Pb based QDs are being investigated. Among these doped QDs (d-dots), based on transition metal ion-doped QDs without heavy metal ions such as wide band gap semiconductors ZnS and ZnSe have attracted considerable attention as the new

generation of luminescence (NCs), can also be used as bio-probes for targeted cancer imaging [13].

ZnS is an important type II–VI semiconductor material because of its luminescent properties. ZnS crystal exists in two phases: one is the cubic phase with a zinc blende (sphalerite) structure; and the other is the hexagonal phase with a wurtzite structure. For the bulk cubic and hexagonal phases of ZnS, the energy gap, E_g is 3.68 eV and 3.80 eV, respectively. At atmospheric pressure, cubic phase ZnS is more stable at low temperatures and transforms to wurtzite ZnS at temperature higher than 1000 °C [14]. Wurtzite ZnS is much more desirable than the cubic phase for its optical properties. Phosphors of ZnS are synthesized in the wurtzite phase to optimize luminescence at a temperature near 1000 °C, because bulk wurtzite crystallizes at temperatures above 1000 °C [15]. It has been shown with thermodynamic analysis using the surface energy data that smaller wurtzite nanoparticles (NP) are thermodynamically more stable than sphalerite [16].

There are few reports on synthesis of wurtzite ZnS (NP) [14,17,18,20]. Zhao et al., reported the synthesis of wurtzite ZnS with size less than 5 nm by heating $ZnCl_2$, tetramethyl-ammonium hydroxide (TMAH) and thiourea in ethylene glycol as the reaction medium at low temperature of 150 °C for 2 h and concluded that polyol plays a key role in forming wurtzite ZnS NCs at low temperatures by using different polyols [17]. It was proposed that polyol forms some intermediates with ZnS which can decompose into wurtzite ZnS at lower temperatures. The exact mechanism of formation of wurtzite ZnS (NP) was explained later by showing that wurtzite ZnO (NP) are formed first as a reaction intermediate which serve as structural templates in the presence of ethylene glycol (EG) for the controllable

* Corresponding authors. Fax: +468 790 9072.

E-mail addresses: rkhan@kth.se (R. Shahid), toprak@kth.se (M.S. Toprak).

formation of wurtzite ZnS [18]. In both cases, the materials they used were toxic and the reaction time was long.

Microwave (MW) irradiation is an emerging efficient heating method, where dielectric heating mechanism involving dipolar polarization and ionic conduction allows faster reactions with higher yields and better purities with no high vacuum requirements. Recently, few groups reported on synthesis of ZnS NCs using MW as heating source [19,20]. Microwave assisted solution based method has been used for low temperature synthesis of shape-controlled nanocrystals with narrow size distribution [21].

Single source molecular precursor decomposition is another technique to synthesize ZnS NCs [14,19,20]. Panda et al. used metal ethyl xanthate to synthesize one dimensional zinc chalcogenide rods and wires by changing the MW irradiation time [19]. Liu reported on synthesis of wurtzite ZnS NCs with the size in the range of 2.8–6.6 nm by thermolysis of single-source molecular precursor (zinc diethyldithiocarbamate, $\text{Zn}(\text{DDTC})_2$) in air at 280 °C for a long reaction time of 12 h [14]. Using the same precursor, synthesis of 5 nm wurtzite ZnS nanoparticles were reported by Sun et al. by MW thermolysis of $\text{Zn}(\text{DDTC})_2$ in EG at 110 °C for a very short time of 5 min, due to high MW absorption of EG [20].

The synthesis of non-toxic QDs using green chemical route is an approach receiving increasing attention recently. There is a need to develop less toxic, low cost method for the synthesis of various functional nanoparticles. In this work we focus on the development of a facile, fast route for synthesis of wurtzite ZnS QDs. MW irradiation was used as heating source in controlled reaction with two different MW absorbing solvents as DMF and EG. The microwave absorption of ethylene glycol is high with loss tangent value 1.35 while microwave absorption of DMF is medium having loss tangent value 0.161, where loss tangent ($\tan\delta = \epsilon''/\epsilon'$) is the ability of a specific solvent to convert microwave energy into heat at a given frequency and temperature [22]. We used both multisource and single source molecular precursors to obtain wurtzite ZnS QDs with different surface capping to make QDs dispersible in hydrophobic or hydrophilic solvents.

2. Experiment

2.1. Materials

All reagents and solvents in the reactions were of analytical grade and used as received, without further purification; zinc chloride powder (ZnCl_2 ; 99.9% Merck), sulfur powder (S_8 ; Reagent grade Aldrich), hexadecylamine [$\text{C}_{16}\text{H}_{35}\text{N}$] (HDA; 90% Aldrich), *n,n*-dimethyl formamide (DMF; 99.8% VWR) [$(\text{CH}_3)_2\text{NC}(\text{O})\text{H}$], zinc diethyldithiocarbamate ($\text{Zn}(\text{DDTC})_2$; 98% Aldrich) $\text{Zn}[(\text{C}_2\text{H}_5)_2\text{NCS}_2]_2$, ethylene glycol (EG; 99.5% Aldrich) [$\text{C}_2\text{H}_4(\text{OH})_2$], thioglycerol (TG; 98% Aldrich) [$\text{HSCH}_2\text{CH}(\text{OH})\text{CH}_2\text{OH}$], hexane [C_6H_{14}] (96.5% Aldrich), methanol [CH_3OH] (99.5% Fluka), ethanol [$\text{C}_2\text{H}_5\text{OH}$] (99.5% Solveco).

The MW system used was Biotage Initiator™ 60 microwave synthesizer operating at a frequency of 2.45 GHz with power output of 0–400 W. The temperature could be varied between 40–250 °C and the pressure 0–20 bar and cavity volume ranging from 0.2 to 20 ml.

2.2. Methods

We developed two different methods using MW absorbing solvents, DMF and EG. Fig. 1 shows the heating profiles of DMF and EG heated for a period of 300 s in 5 ml reaction cavity. EG being strong MW absorbing solvent can be heated safely to 200 °C in 100 s in 5 ml reaction cavity, due to high pressure build up, while DMF can be heated up to 250 °C. Once the desired temperature is attained inside the MW cavity, it remains uniform throughout the reaction as can be seen from temperature profile

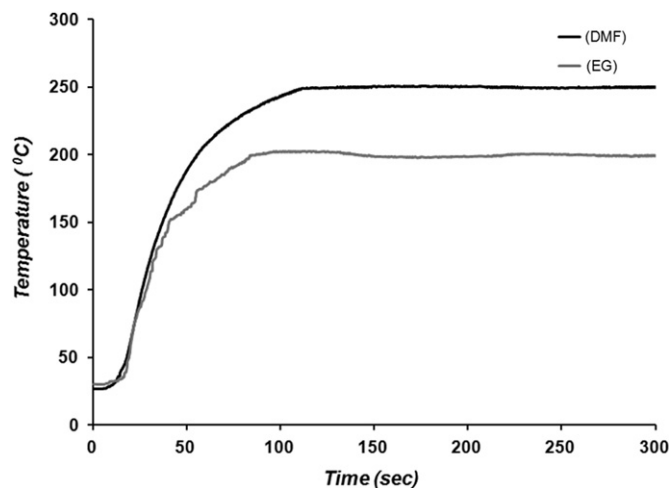


Fig. 1. Temperature profiles of DMF and EG heated for 300 s.

of solvents shown in Fig. 1. The reaction time and temperature of the two systems were optimized to obtain QDs with high yield of reaction at low reaction temperature and short reaction time. Temperature was varied from 150 °C to 250 °C for DMF and the temperature range selected for EG was between 100 °C and 200 °C. A series of experiments with 10 °C intervals have been performed. Effect of different reaction temperatures and times were investigated on the quality, quantity and size of ZnS QDs. This was qualitatively assessed from the position and intensity of the UV–Vis absorption peak and also confirmed by TEM analysis.

Multisource precursors were used in DMF while single source precursor was used in EG; the two methods are referred to as MS-DMF and SS-EG, respectively. HDA was used as capping agent for MS-DMF and TG for SS-EG. Equal concentration of zinc and sulfur source i.e., zinc chloride and sulfur powder in DMF was used for MS-DMF and single molecular precursor $\text{Zn}(\text{DDTC})_2$ was used in EG for SS-EG. Concentration of capping agent was 10 times the concentration of metal source in both cases. The total volume of both solutions was 5 ml.

In the first method (MS-DMF), ZnCl_2 (1 mmol) and sulfur powder (1 mmol) were added to DMF (2 ml) with HDA (0.01 mol). The solution was preheated in a water bath to 70 °C until it became clear then was irradiated by MW at 150 °C for 60 s under continuous stirring. Methanol was added to precipitate the QDs from the solution. The product was centrifuged and re-dispersed in a hydrophobic solvent, i.e., hexane.

In the second method (SS-EG), $\text{Zn}(\text{DDTC})_2$ (0.5 mmol) and TG (5 mmol) was added into EG (5 ml). The solution was heated to 150 °C by MW irradiation for 300 s under stirring and cooled to room temperature. The QDs were separated by centrifugation and washed with ethanol. The QDs were finally dispersed in a hydrophilic solvent, i.e., ethanol.

The size and morphology of QDs was characterized by HR-TEM JEM 2100F microscope equipped with field emission gun. For specimen preparation, a drop from the suspension of the QDs readily dispersible in respective solvent without any ultrasonic sonication was placed on 5 nm carbon coated copper grid. The crystalline phase of the QDs was analyzed from selected area electron diffraction (SAED) patterns.

Optical absorption of the samples was measured by using Perkin–Elmer–Lambda 750 UV–VIS spectrometer. The samples were dispersed in respective solvent while pure solvent was used as reference and the spectra were recorded from 200 to 500 nm. The PL spectrum was recorded using Perkin–Elmer (LS 55) fluorescence spectrometer. The samples were dispersed in respective solvents and the spectra were recorded from 300 to 600 nm.

3. Results and discussion

The QDs obtained from the two methods are shown in TEM images in Fig. 2(a) and (b) and HRTEM images in Fig. 2(c) and (d). Due to low contrast of ZnS it is difficult to exactly determine the size of the particles. The estimated size of the ZnS QDs obtained from measuring at least 300 QDs from various TEM images is 2.2 ± 0.1 nm and 2.4 ± 0.3 nm synthesized with methods MS-DMF and SS-EG, respectively.

Fig. 2(e) and (f) are the SAED patterns of ZnS QDs synthesized by method MS-DMF and SS-EG, respectively with diffraction rings indexed to (1 0 1) (1 0 3) and (2 0 1) crystal planes of the wurtzite structure of ZnS (JCPDS No. 001-0677). The SAED pattern of ZnS QDs show diffraction rings instead of sharp spots due to small size of QDs. FFT performed on randomly selected individual particles from HRTEM images also revealed d -spacing of planes matching to wurtzite structure of ZnS QDs as shown in Fig. 2(c) and (d).

The method of sample preparation can have a decisive influence on the reaction path and thereby the properties of the synthesis products. We synthesized wurtzite ZnS QDs by using EG and DMF as MW absorbing reaction medium and because of high MW absorption of solvents it was possible to make wurtzite ZnS QDs at low temperature.

Optical properties of the QDs were investigated by UV–Vis absorption and photoluminescence (PL) spectroscopy. The QDs synthesized by the two methods show strong UV absorption onset at 350 nm with a shoulder at 320 nm for MS-DMF and a

weak shoulder at 313 nm for SS-EG as shown in Fig. 3, which is slightly blue shifted from the absorption of bulk wurtzite ZnS. This blue shift in absorption is due to quantum confinement effect resulted from the small size of ZnS quantum dots when the radius of QDs is comparable to excitonic Bohr radius a_B^{exc} of bulk ZnS. Following equation can be used to calculate a_B^{exc} for wurtzite form of bulk ZnS [23]

$$a_B^{\text{exc}} = 0.529 \varepsilon_{\infty} \left(\frac{1}{m_e^* m_0} + \frac{1}{m_h^* m_0} \right) \quad (1)$$

where ε_{∞} is the high-frequency relative dielectric constant while m_e^* and m_h^* are the effective masses of the electron and hole, respectively and m_0 is the rest mass of the electron. For the bulk wurtzite ZnS structure ($m_e^*=0.28$, $m_h^*=0.5$, and $\varepsilon_{\infty}=5.2$) [24], Eq. (1) gives a_B^{exc} of 1.5 nm which correspond to diameter of 3 nm. QDs size estimated from TEM images, as 2.2 ± 0.1 nm and 2.4 ± 0.3 nm for SS-DMF and MS-EG, respectively, along with the observed absorption characterization strongly suggests the quantum confinement.

The Photoluminescence spectra of QDs were recorded using an excitation wavelength of 330 nm. The QDs synthesized by method MS-DMF show a broad emission peak centered at 435 nm while QDs prepared by SS-EG show a narrower emission peak at 370 nm as shown in Fig. 3. For ZnS the valence band consists largely of s and p orbitals from sulfur while the conduction band is mainly due to s states of zinc [25]. Four types of point defects can be present in pure ZnS particles. Vacancies of sulfur and zinc are

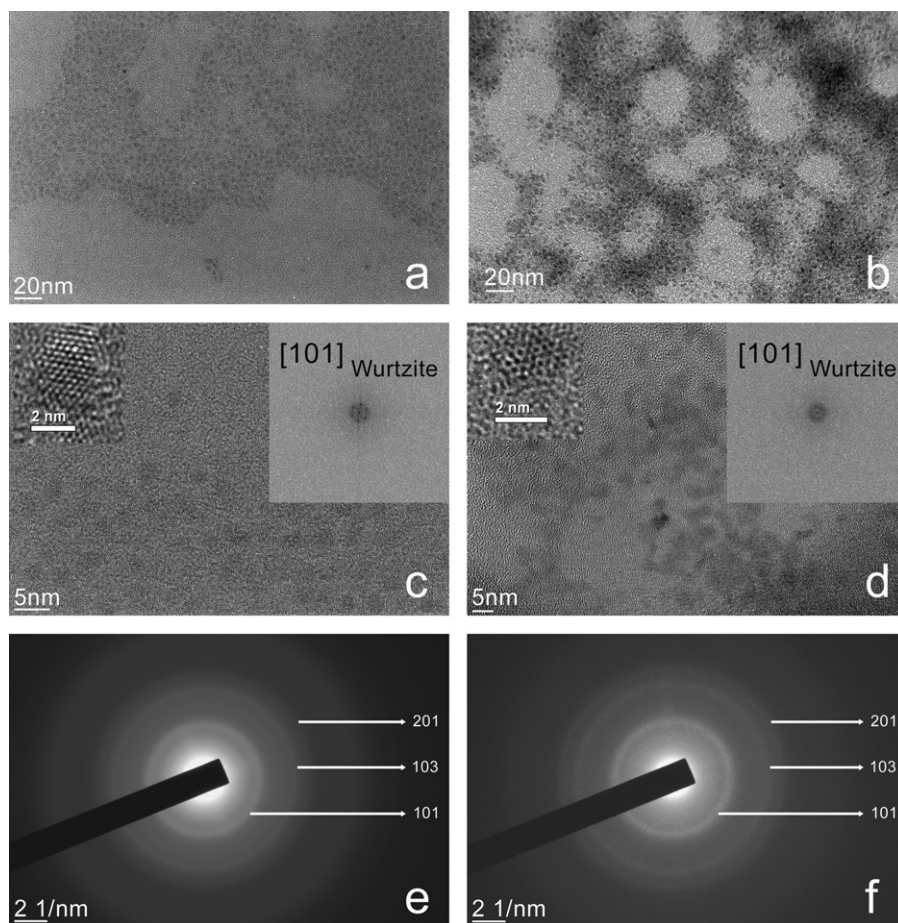


Fig. 2. TEM images of ZnS QDs synthesized by MS-DMF (a) and (c) and SS-EG (b) and (d). Insets in (b) and (d), are HRTEM images of QDs and FFT performed on individual QDs. (e) and (f) SAED patterns of ZnS QDs.

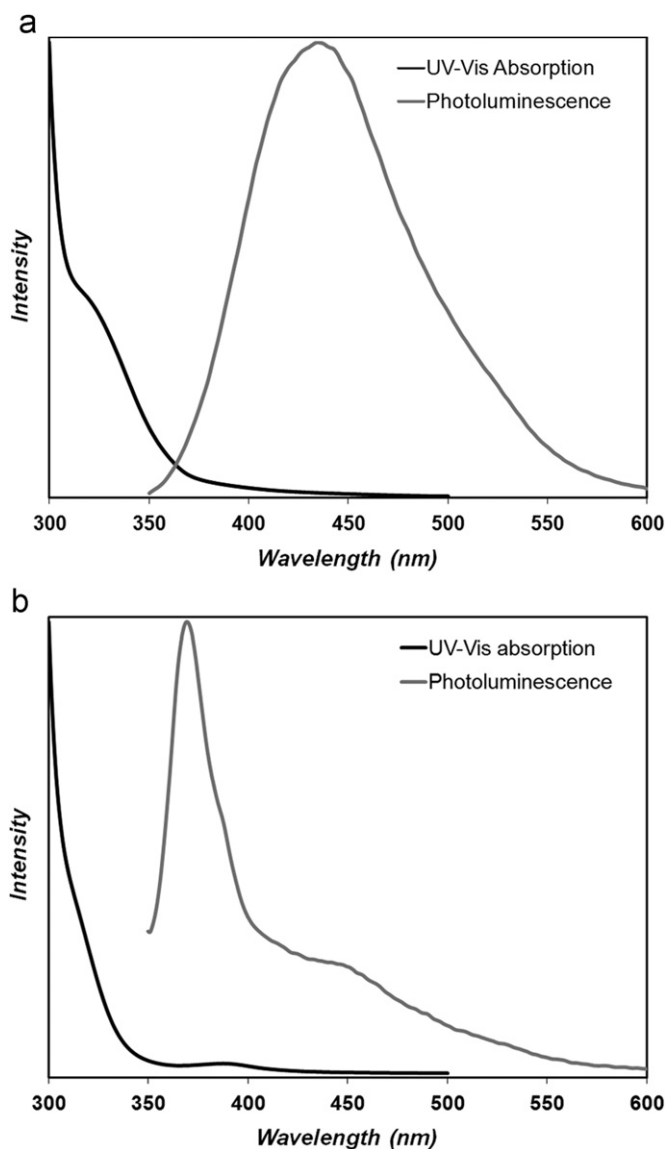


Fig. 3. UV-Vis absorption and PL spectra of ZnS QDs synthesized by method MS-DMF (a) and SS-EG (b).

equivalent to localized donor and acceptor states, respectively. In the case of interstitials, zinc atoms lead to donor states and sulfur atoms to acceptor states. Vacancy states lie deeper in the gap than states arising from interstitial atoms [26].

The broad PL emission of QDs from method MS-DMF is attributed to the transitions originating from sulfur vacancies [25,27]. However, the narrow emission from ZnS QDs synthesized by method SS-EG is attributed to the band edge emission.

4. Conclusion

Wurtzite ZnS QDs with size less than 3 nm were synthesized by low temperature, simple, fast, and less toxic synthesis method using MW energy as the heating source. We used both multi-source and single source precursors in MW absorbing solvents using different capping agents to obtain well separated wurtzite ZnS QDs to be dispersed in different media to allow their use in different applications. The quantum confinement effect is observed in the optical properties of QDs related to their small size. The presented methods are facile and can be used for synthesis of other semiconductor nanocrystals.

Acknowledgments

We thank Dr. Wubeshet Sahle for his help in TEM analysis, Higher Education Commission of Pakistan and Swedish Research Council for providing funding for this work.

References

- [1] G.P.C. Drummen, *Int. J. Mol. Sci.* 11 (2010) 154–163.
- [2] Y. Kayanuma, *Phys. Rev. B* 38 (1988) 9797–9805.
- [3] R. Rossetti, S. Nakahara, L.E. Brus, *J. Chem. Phys.* 79 (1983) 1086–1088.
- [4] R. Rossetti, J.L. Ellison, J.M. Gibson, L.E. Brus, *J. Chem. Phys.* 80 (1984) 4464–4469.
- [5] R. Rossetti, R. Hull, J.M. Gibson, L.E. Brus, *J. Chem. Phys.* 82 (1985) 552–559.
- [6] C.B. Murray, D.J. Norris, M.G. Bawendi, *J. Am. Chem. Soc.* 115 (1993) 8706–8715.
- [7] A.P. Alivisatos, *Science* 271 (1996) 933–937.
- [8] Z.A. Peng, X. Peng, *J. Am. Chem. Soc.* 123 (2001) 183–184.
- [9] Y.A. Yang, H. Wu, K.R. Williams, Y.C. Cao, *Angew. Chem. Int. Ed.* 44 (2005) 6712–6715.
- [10] N. Pradhan, D. Reifsnnyder, R. Xie, J. Aldana, X. Peng, *J. Am. Chem. Soc.* 129 (2007) 9500–9509.
- [11] L. Li, T.J. Daou, I. Texier, T.T.K. Chi, N.Q. Liem, P. Reiss, *Chem. Mater.* 21 (2009) 2422–2429.
- [12] C. Wang, X. Gao, X. Su, *Anal. Bioanal. Chem.* 397 (2010) 1397–1415.
- [13] K. Manzoor, S. Johnny, D. Thomas, S. Setua, D. Menon, S. Nair, *Nanotechnology* 20 (2009) 065102.
- [14] W. Liu, *Mater. Lett.* 60 (2006) 551–554.
- [15] Z. Wang, L.L. Daemen, Y. Zhao, C.S. Zha, R.T. Downs, X. Wang, Z.L. Wang, R.J. Hemley, *Nat. Mater.* 4 (2005) 922–927.
- [16] H. Zhang, F. Huang, B. Gilbert, J.F. Banfield, *J. Phys. Chem. B* 107 (2003) 13051–13060.
- [17] Y. Zhao, Y. Zhang, H. Zhu, G.C. Hadjipanayis, J.Q. Xiao, *J. Am. Chem. Soc.* 126 (2004) 6874–6875.
- [18] F. Dawood, R.E. Schaak, *J. Am. Chem. Soc.* 131 (2009) 424–425.
- [19] A.B. Panda, G. Glaspell, M.S. El-Shall, *J. Am. Chem. Soc.* 128 (2006) 2790–2791.
- [20] J.Q. Sun, X.P. Shen, K.M. Chen, Q. Liu, W. Liu, *Solid State Commun.* 147 (2008) 501–504.
- [21] L.X. Yang, Y.J. Zhu, H. Tong, W.W. Wang, G.F. Cheng, *J. Solid State Chem.* 179 (2006) 1225–1229.
- [22] D. Dallinger, C.O. Kappe, *Chem. Rev.* 107 (2007) 2563–2591.
- [23] A.V. Dijken, A.H. Janssen, M.H.P. Smitsmans, D. Vanmaekelbergh, A. Meijerink, *Chem. Mater.* 10 (1998) 3513–3522.
- [24] B. Segall, *Phys. Rev.* 163 (1967) 769–778.
- [25] W.G. Becker, A.J. Bard, *J. Phys. Chem.* 87 (1983) 4888–4893.
- [26] D. Denzler, M. Olschewski, K.J. Sattler, *Appl Phys.* 84 (1998) 2841–2845.
- [27] S. Wageh, Z.S. Ling, X.X. Rong, *J. Cryst. Growth* 255 (2003) 332–337.